A GRID CONNECTED PHOTOVOLTAIC GENERATION SYSTEM WITH COMPENSATION OF CURRENT HARMONICS AND VOLTAGE SAGS

Marcelo Cabral Cavalcanti, Gustavo Medeiros de Souza Azevedo, Bruno de Aguiar Amaral
Francisco de Assis dos Santos Neves, Davi Carvalho Moreira, Kleber Carneiro de Oliveira
Departamento de Engenharia Elétrica e Sistemas de Potência – Universidade Federal de Pernambuco
CEP 50.740-530, Recife - PE
Brasil
e-mail: marcelo.cavalcanti@ufpe.br, gustavo.azevedo@ufpe.br, fneves@ufpe.br, kleber.oliveira@ufpe.br

***Abstract* – This paper presents a system that provides photovoltaic generation as well as the ability to compensate current harmonics and voltage sags. The system can be controlled for current harmonics and reactive power compensation simultaneously by using a converter operating as shunt active filter. Another converter is used as active series filter and it compensates voltage harmonics and voltage sags and swells. Using only one dc-ac converter in photovoltaic energy conversion process, the system presents increased efficiency when compared to the conventional systems, composed by a dc-dc converter and a dc-ac converter. The synchronous reference frame method is used to control the three-phase converters. Simulation results demonstrate the good performance of the proposed configuration. Experimental results corresponding to the operation of the series filter as voltage sag compensator are presented.**

***Keywords* – Converter control, Power Quality, Renewable energy systems, Solar Cell Systems, Three phase systems, Vector control.**

I. INTRODUCTION

Photovoltaic (PV) energy has great potential to supply energy with minimum impact on the environment, since it is clean and pollution free [1]. A large number of solar cells connected in series and parallel set up the PV or solar arrays. One way of using photovoltaic energy is in a distributed energy system as a peaking power source [2].

On the other hand, strict regulations have been applied to allow any equipment to be connected to the utility lines. Some of these regulations are related to harmonics distortion and power factor. However, with the use of power electronics, much equipment tends to increase the levels of harmonic distortion. The line current at the input of a diode bridge rectifier deviates significantly from a sinusoidal waveform and this distorted current can also lead to distortion in the line voltage. Moreover, most modern equipments use digital controllers, based on microprocessors which are sensitive to distortions in the voltage and current waveforms. Therefore, in order to improve the PV system utilization, the power conversion can be designed to also provide the functions of a Unified Power Quality Conditioner (UPQC).

The utilization of two connected back-to-back, dc-ac fully controlled converters gives the system the most versatile structure of converters applied for energy conditioning. In this case, depending on the control scheme, the converters can have different functions of compensation. For instance, they can behave as active series and shunt filters combined to compensate simultaneously load current and supplied voltage harmonics [3]. In this way, the equipment is called UPQC [4] and many papers have discussed about the functions of the UPQC [5-15]. The objective of this paper is to propose the grid connection of the PV array trough the dc-link of a fully controlled ac-dc-ac converter. Using this configuration, the converters can be controlled to simultaneously maximize the PV output power and accomplish the functions of a UPQC.

An active shunt filter is a suitable device for current-based compensation [16]. This configuration includes current harmonics and reactive power compensation. The active series filter is normally used for voltage-based compensation [16]. In this case, voltage harmonics and voltage sags and dips are compensated.

Other applications can be found in literature, such as reactive power compensation, active power control and voltage regulation. In this case, it is called Unified Power Flow Controller (UPFC) [17]-[18].

Conventionally, grid connected PV energy conversion systems are composed of a dc-dc converter and a dc-ac converter (active shunt filter) [1]-[2]. The dc-dc converter is controlled to track the maximum power point of the photovoltaic array and the dc-ac converter is controlled to produce current in such a way that the system current has low total harmonic distortion (THD) and it is in phase with the utility voltage. The efficiency of the conventional system is low because the dc-dc converter and the inverter are connected in series. The proposed system eliminates the need of the dc-dc converter and increases the conversion efficiency, as shown in [19]. Using a dc-dc converter and a dc-ac converter, the efficiency is at most 90% while without using the dc-dc converter the efficiency is around 94%. One of the dc-ac converters operates as power supply as well as harmonic and reactive power compensator when the sun is available. At low irradiation, the system operates only as harmonics and reactive power compensator. The other dc-ac converter is used to provide voltage harmonics and voltage sag compensations. Cost estimation shows that the use of the additional components needed for power quality improvements increases the cost in less than 12%. Also this

Manuscript received on May 11, 2005; first revision August 20, 2005; second revision on March 3, 2006. Recommended by the Editor of the Special Section Edson H. Watanabe.

additional converter does not change the efficiency of the PV energy conversion since the converters are connected in parallel. The control was implemented with the synchronous reference frame method. The system and controllers were designed and simulated. Different pulse-width-modulation (PWM) techniques have been compared to suggest a configuration with optimal performance. The system provides approximately 2.8 kW of photovoltaic generation.

II. GRID CONNECTED PHOTOVOLTAIC SYSTEM

The proposed photovoltaic (PV) energy conversion system has high efficiency, low cost and high functionality. Figure 1 shows the block diagram of the proposed system. The converter 1 (PV converter) in Fig. 1 is responsible for converting the PV energy with Maximum Power Point Tracking (MPPT) as well as for compensating current harmonics and reactive power. The converter 2 (Dynamic Voltage Restorer – DVR converter) in Fig. 1 is responsible to compensate voltage harmonics and voltage sags.

The steady state fundamental components are sinusoidal in the *abc* frame. To reduce the control complexity, the d-q frame rotating at the supply frequency can be used. With this reference frame the positive-sequence components at fundamental frequency become constant [20]. To achieve better control performance, a fast internal loop and a slow external loop are used. The current and voltage controls are achieved by using PI compensators. The Phase-Locked-Loop (PLL) circuit detects amplitude and position of the supply voltage vector.

III. MAXIMUM POWER POINT TRACKING

Figure 2 shows the control block diagram of converter 1 in Fig. 1.

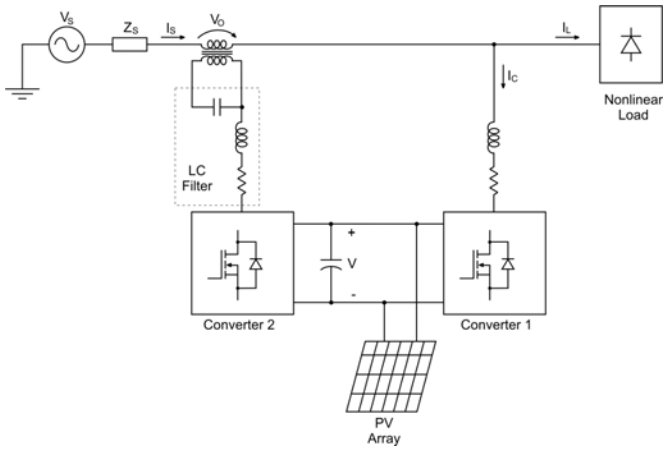

Fig. 1. Proposed system: PV generation with UPQC function.

It has to track the maximum power point of the photovoltaic array as well as to compensate current harmonics and reactive power. When the system is operating as photovoltaic energy generator, the MPPT controller is used to calculate the reference voltage. When the system is operating only as harmonic and reactive power compensator, the reference voltage is constant [1].

It is important to operate the photovoltaic system near the maximum power point to increase the efficiency of photovoltaic arrays. A MPPT scheme often used is the perturbation and observation method [21]. However, in this paper, the slope of power versus voltage curve is used, which decreases the oscillation problem and it is easy to implement [1]. The output power of the PV array and the derivative of the output power to the output voltage can be expressed as

$$P = V \cdot I \tag{1}$$

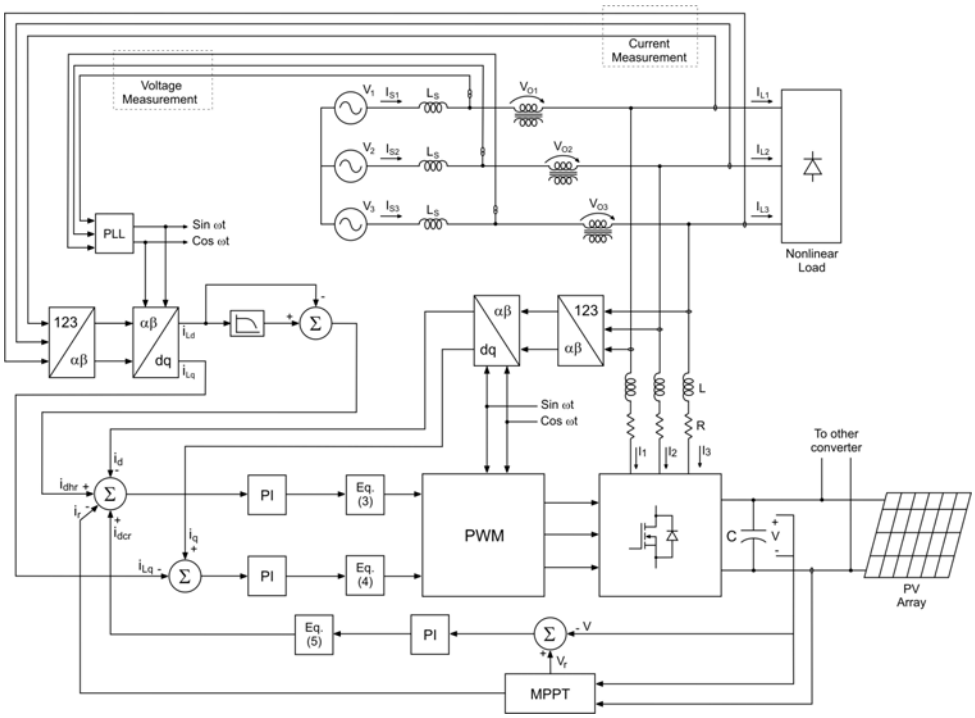

Fig. 2. Control of the proposed system: PV generation / current harmonics and reactive power compensations.

$$\frac{dP}{dV} \cong I + \frac{\Delta I}{\Delta V} \cdot V \qquad (2)$$

Where:

P - PV array output power.
V - PV array output voltage.
I - PV array output current.
ΔI - Increment of the PV array output current.
ΔV - Increment of the PV array output voltage.

In the method, (2) is used as the index of the maximum power point tracking operation (Fig. 3), where *S* is the solar irradiation. When *dP/dV<0*, decreasing the reference voltage forces *dP/dV* to approach zero; when *dP/dV>0*, increasing the reference voltage forces *dP/dV* to approach zero; when *dP/dV=0*, reference voltage does not need any change [1].

The complete system shown in Fig. 1 was represented in Matlab and the performances of the MPPT scheme, active shunt filter and DVR during the voltage sag were verified. A short circuit in the power system, causing a voltage sag in V_S was considered to occur from 0.02s to 0.12s. All simulation results presented in this paper correspond to the operation of the system in Fig. 1 during this disturbance. The reference voltage generated by the MPPT algorithm has small oscillation around the ideal voltage at the beginning and the end of the short circuit (Fig. 4). The PV array voltage stays near to the ideal voltage that is around 121V. Even during the voltage sag, the MPPT algorithm presents very good results with at least 99% of the PV maximum output power.

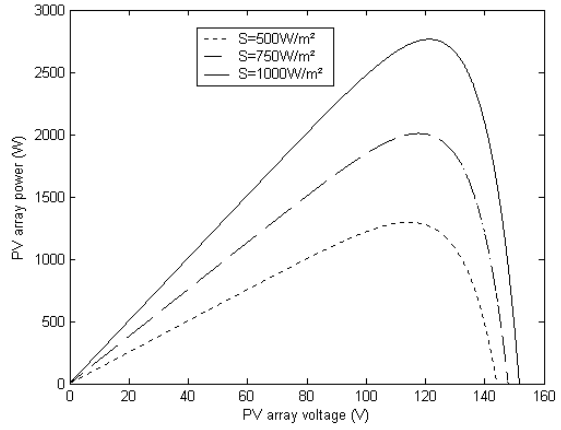

Fig. 3. Characteristic diagram of the solar array.

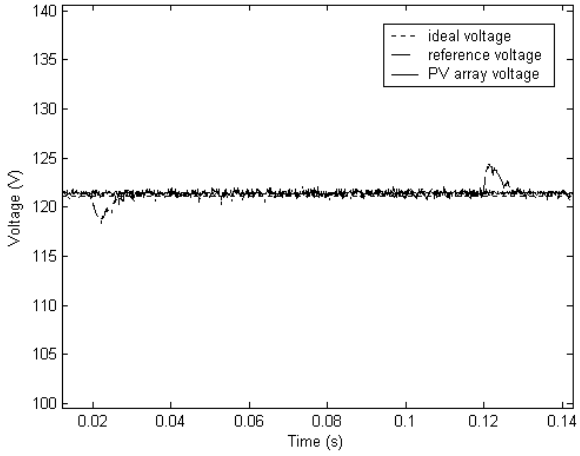

Fig. 4. MPPT controller: solar array output voltage.

IV. CURRENT BASED COMPENSATION

In the supply voltage vector oriented reference frame, the fundamental frequency positive-sequence components appear as dc quantities [20]. Since the supply currents must have sinusoidal waveforms and be in phase with the utility voltages in the proposed design, the supply current vector has only d-axis component. Therefore, the q-axis reference current for the inverter is the q-axis load current [2]. The d-axis reference current is composed of three parts: reference d-axis load current (i_{dhr}), reference dc link current (i_{dcr}) and reference photovoltaic array current (I_r). The d-axis load current is passed through a low pass filter that removes the high frequency components in the d-q reference frame. A first order low pass filter with a cut frequency of 20Hz is used. Subtracting the d-axis load current from the filtered d-axis load current, the result is the negative of the d-axis harmonics. This value is used as the reference d-axis load current since the positive current flows into the inverter.

The dc current component in the d-q reference frame corresponds to the fundamental component of the real power flowing to the load. The inverter dc link voltage controller calculates the current necessary to maintain the dc link voltage by passing the dc link voltage error through a PI compensator. The current obtained by the MPPT controller corresponds to the real power available from the photovoltaic array and it is subtracted from the other current components.

The modeling and control of the system is based on the development presented in reference [20] and equations (3), (4) and (5) in Fig. 2 are

$$v_{nd} = \frac{v_d + \omega \cdot L \cdot i_q - u_d}{V} \qquad (3)$$

$$v_{nq} = \frac{v_q - \omega \cdot L \cdot i_d - u_q}{V} \qquad (4)$$

$$i_{dcr} = \frac{2 \cdot V \cdot u_{dc}}{3 \cdot V_{grid}} \qquad (5)$$

Where:

v_{nd} - D-axis normalized reference voltage (converter 1).
v_{nq} - Q-axis normalized reference voltage (converter 1).
v_d - D-axis grid voltage.
v_q - Q-axis grid voltage.
ω - System angular frequency.
L - Inductance of the matching transformer.
u_d - D-axis output of the current PI compensator.
u_q - Q-axis output of the current PI compensator.
u_{dc} - Output of the voltage PI compensator.
V_{grid} - Amplitude of the grid voltage.

Using the voltage vector oriented d-q reference frame, the coupled dynamics of the current tracking problem have been transformed into decoupled dynamics. By adjusting PI compensators, a fast tracking and zero steady state errors can be achieved. The results (Fig. 5 and Fig. 6) show that the oscillating current harmonics injected by the inverter track their references with high accuracy even during the voltage sag. The dc link current increases, and so does the d-axis current component, to keep the maximum power in PV array.

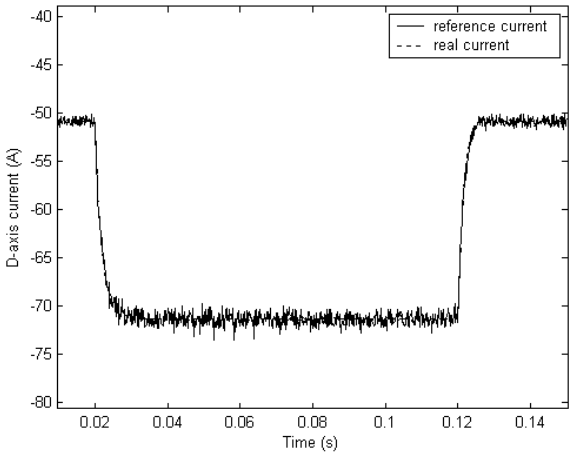

Fig. 5. Tracking performance of the d-axis current loop.

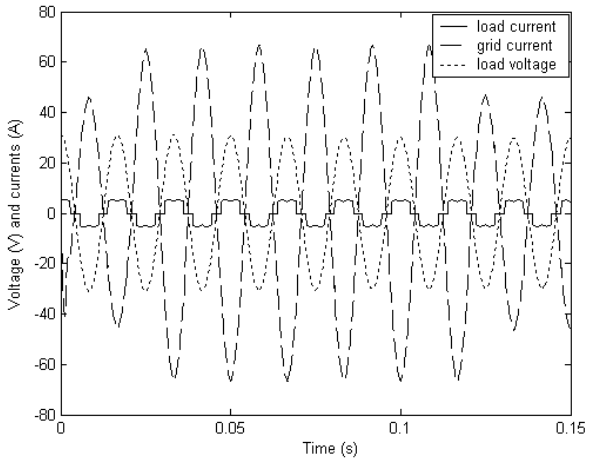

Fig. 7. Current harmonics and reactive power compensations.

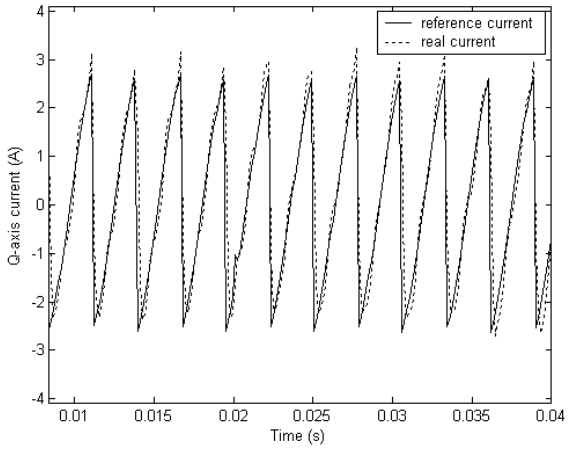

Fig. 6. Tracking performance of the q-axis current loop.

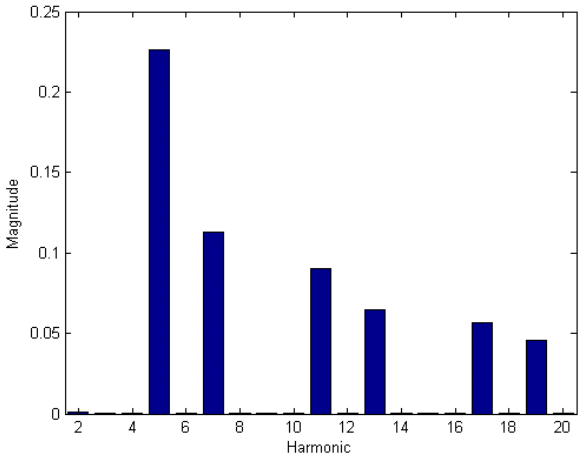

Fig. 8. Load current harmonics components.

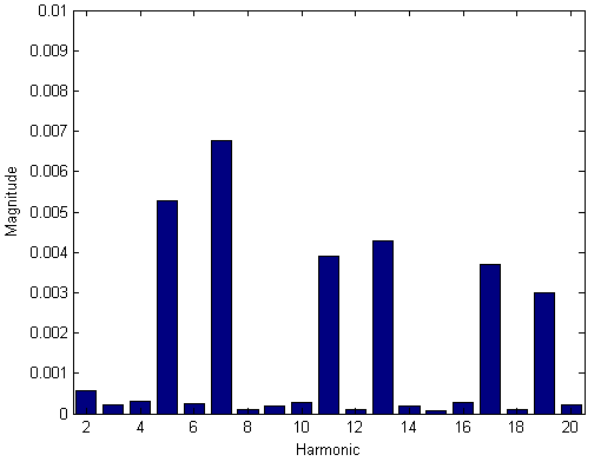

Fig. 9. Supply current harmonics components.

The controller can compensate harmonics and reactive power effectively as shown in Fig. 7. The supply current and the load voltage are displaced by 180^0 because it is generated more power from the PV array than that needed for the load. Therefore, in this case the PV array supplies the load and injects power into the system. It can be also seen that the amplitude of the grid current increases from 46A to 67A because of the voltage sag from 0.02s to 0.12s. The increase in the grid current means that the energy to supply the load during the voltage sag comes from the PV array since the grid current and the load voltage are displaced by 180^0. Figures 8 and 9 present the load and supply current harmonics components normalized by the fundamental component, which is not shown to allow a better visualization of the harmonics components.

V. VOLTAGE BASED COMPENSATION

Figure 10 shows the controller block diagram of converter 2 in Fig. 1. The voltage compensator is a system based on power electronics that detects the feeder voltage and in case the voltage is different of the desired voltage, it supplies the necessary voltage to compensate the voltage error. It can be used to compensate voltage harmonics at the point of common coupling and voltage sags, keeping the load voltage around its rated value.

In this paper, it is presented the voltage sag compensation control. Its use is more justified when many sensitive loads are connected to the same feeder [22].

The system modeling and control are developed and equations (6) and (7) in Fig. 10 are

$$v_{nd2} = \frac{v_{od} - \omega \cdot L_c \cdot i_{cq} + u_{d2}}{V} \qquad (6)$$

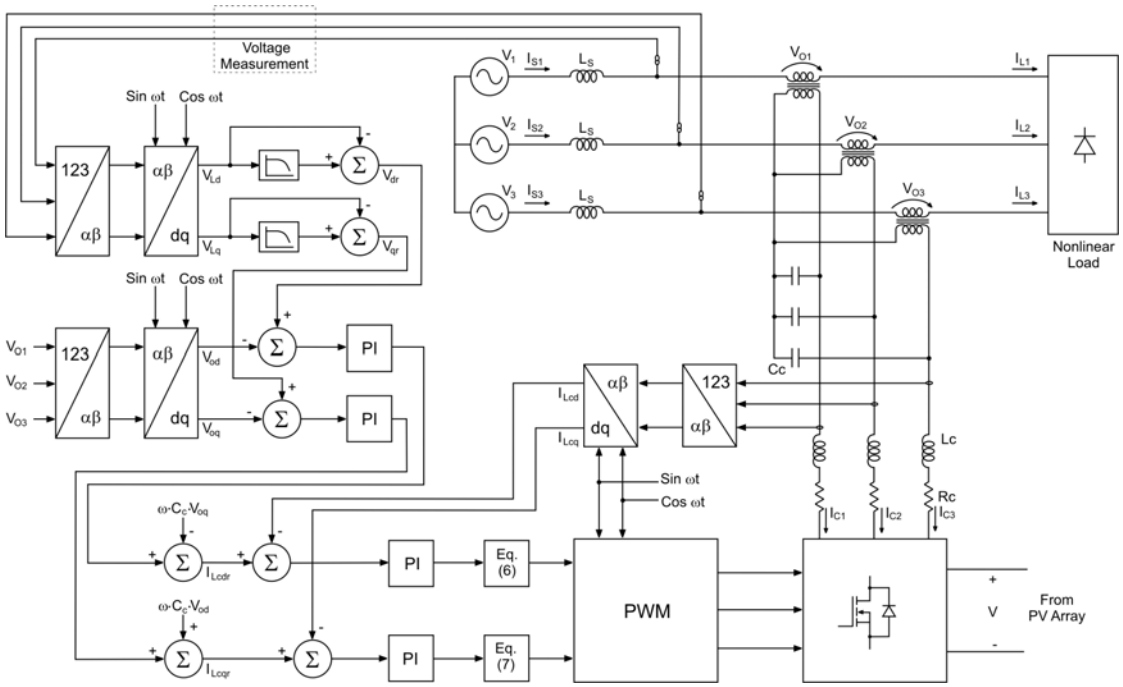

Fig. 10. Control of the proposed system: voltage sag compensation.

$$v_{nq2} = \frac{v_{oq} + \omega \cdot L_c \cdot i_{cd} + u_{q2}}{V} \tag{7}$$

Where:

- v_{nd2} - D-axis normalized reference voltage (converter 2).
- v_{nq2} - Q-axis normalized reference voltage (converter 2).
- v_{od} - D-axis injected voltage.
- v_{oq} - Q-axis injected voltage.
- L_c - Inductance of the filter.
- u_{d2} - D-axis output of the current PI compensator.
- u_{q2} - Q-axis output of the current PI compensator.

The voltage sag compensator (or DVR) is composed basically of an energy storage system, a dc-link, a dc-ac converter and a transformer (Fig. 1).

To find out which is the load reference voltage when voltage sag occurs, it is necessary to determine the voltage value before the sag. The output signals of a PLL are used to inform in a very short time the values of V_d, V_q and θ. During voltage sags, the variations in the angle θ originate another synchronous referential rotated in relation to the original reference angle θ* (Fig. 11).

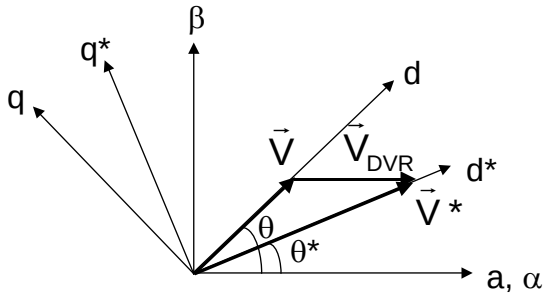

Fig 11. Reference axes system during a voltage sag.

One of the methods for generating the reference voltage consists of using a low pass filter in the output signals of the PLL. This filter has a slow dynamic response, in such a way that the difference between the reference signal and the supply signal is the voltage value that should be injected by the DVR to compensate the sag.

$$\begin{aligned} \Delta V_d &= V_d^* - V_d \\ \Delta V_q &= V_q^* - V_q \end{aligned} \tag{8}$$

From Fig. 11,

$$\begin{aligned} V_{DVR,d} &= V_d^* - V\cos\left(\theta - \theta^*\right) \\ V_{DVR,q} &= V_q^* - V\,sin\left(\theta - \theta^*\right) \end{aligned} \tag{9}$$

Knowing that V_q* should be zero, (9) is simplified for

$$\begin{aligned} V_{DVR,d} &= V_d^* - V\cos\left(\theta - \theta^*\right) \\ V_{DVR,q} &= -V\,sin\left(\theta - \theta^*\right) \end{aligned} \tag{10}$$

Where:

- V_d^* - D-axis load reference voltage.
- V_q^* - Q-axis load reference voltage.
- V_d - D-axis grid voltage.
- V_q - Q-axis grid voltage.
- $V_{DVR,d}$ - D-axis DVR reference voltage.
- $V_{DVR,q}$ - Q-axis DVR reference voltage.
- V - Grid voltage vector.
- θ - Grid voltage vector angle.
- θ^* - Load reference voltage vector angle.

To determine the value of the reference angle θ*, instead of filtering the angle θ that is supplied by the PLL, it should be filtered the value of ω*. The output of this filter passes through an integer, supplying the reference angle.

A. Simulation Results

The controller can compensate voltage sags effectively as shown in Fig. 12, which presents the phase 1 supply and load voltages. Phases 2 and 3 also present effective compensation, and rated voltage values are supplied to the load.

B. Experimental Results

The prototype of the DVR is composed of a controlled rectifier (this converter will be used as the shunt active filter in the future) plus an input filter, a capacitor set (dc link), an inverter, an output filter and a series transformer. The prototype of the DVR was built as an intermediate step in the process of construction of the whole system. Figure 13 shows the picture of the experimental system.

It is also included a three-phase resistive load. The experimental tests have been realized with approximately 200V (line-to-line rms voltage). The control system consists of a microcomputer with interfaces dedicated to measure the electrical variables and to command the converter switches.

The DVR can be optimally designed according to the criteria proposed in [23]. For the experimental results shown in this paper, the parameters of the DVR are:

1. Input filter: 1.8mH, 10A
2. Rectifier and inverter: 6 switch + diode (1200V, 50A)
3. Dc-link capacitance: 4.7mF, 900V
4. Output filter: 5mH and 40μF
5. Series transformer: 3 single-phase (220V:220V)

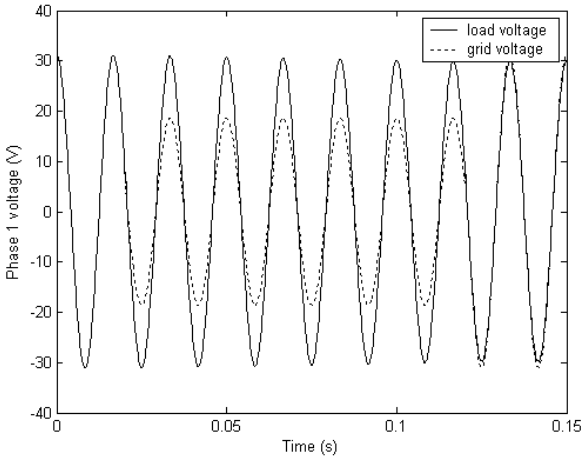

Fig. 12. Phase 1 voltages during the simulation.

Fig. 13. Picture of the experimental system.

Figure 14 shows the three-phase supply and load voltages demonstrating the DVR is capable of compensating a three-phase voltage sag.

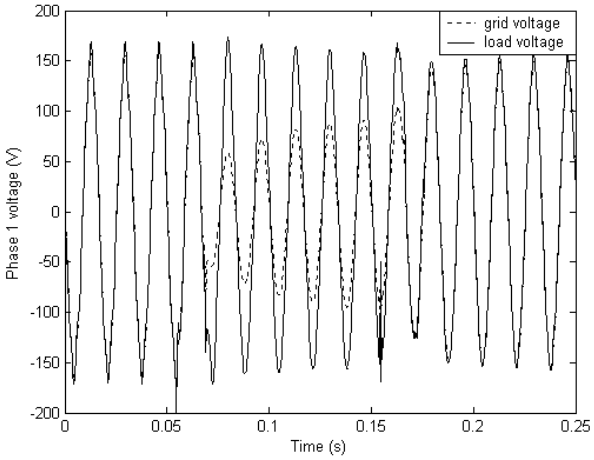

(a) Phase 1

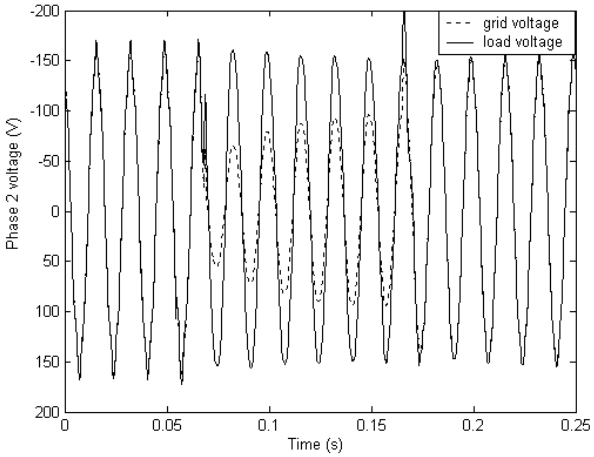

(b) Phase 2

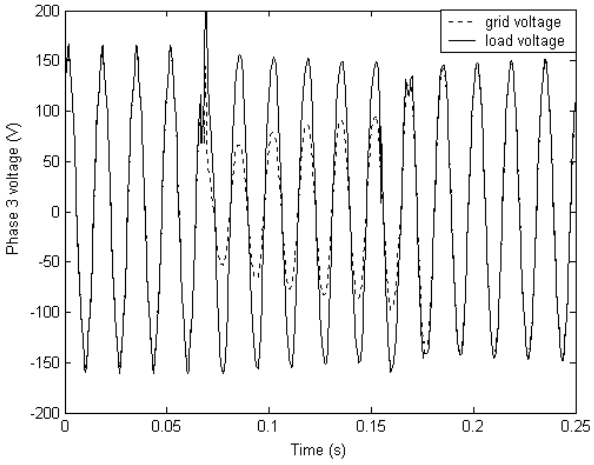

(c) Phase 3

Fig. 14. Three-phase voltages during the experiment.

VI. PWM TECHNIQUES

Space vector modulation (SVM) is nowadays the most used PWM technique in voltage source inverters. SVM is based on the concept of approximating a rotating reference voltage space vector with those on a three-phase inverter.

An optimal pulse-width-modulation is obtained on a voltage second average basis if only the vectors adjacent to the reference vector are used (SVPWM). In this case each phase is switched in sequence by switching only one inverter leg at each transition from one state to the next one. One possibility to reduce the number of switching is to use the two-phase modulation in which only two phases are modulated while the third phase is clamped to the positive (DPWMMAX) or negative (DPWMMIN) dc rail [24]. Since clamping implies in no switching losses, this technique reduces losses in each modulation interval.

SVM techniques can also be implemented by using digital scalar PWM. In this approach, non-sinusoidal modulating waveforms are introduced in a simple way. In digital scalar PWM the split and distribution of the zero space vectors duration $V_0(t_{01})$ and $V_7(t_{02})$, inside the sampling interval, can be represented by the apportioning factor $\mu = t_{01} / (t_{01} + t_{02})$ [25]. When $0 < \mu < 1$, the modulation is known as continuous modulation. The case μ=0.5 is equivalent to SVPWM. When $\mu = 0$ (DPWMMAX) or $\mu = 1$ (DPWMMIN) the modulation is known as discontinuous modulation.

Because of the simple implementation, the digital scalar PWM is used in this paper to control the inverters. The normalized reference voltages in (3), (4), (6) and (7) are transformed to normalized reference phase voltages.

To verify the design of the proposed conversion system, simulations using different loads were realized. Inverter efficiencies have been calculated from the component models used with curve fitting techniques [26] for different load conditions. DPWMMIN and DPWMMAX present the best efficiencies among the PWM techniques. It is expected since only two phases are modulated at each modulation interval for those techniques. The MPPT algorithm presents very good results with at least 99% of the PV maximum output power. The Total Harmonic Distortion (THD) of the supply currents is kept below 5% for all situations. The sinusoidal PWM (SPWM) presents the highest THD content.

Based on characteristics discussed above, the criteria to be used to compare PWM techniques for the PV conversion system is the inverter efficiency since the differences among the MPPT efficiencies are very small when changing the PWM technique. Also, except for the SPWM, the differences among the THD of the system currents are very small when changing the technique. Therefore for the proposed design, DPWMMIN or DPWMMAX should be used to control the switches in the converters 1 and 2 to improve efficiency.

VI. COST ESTIMATION

The proposed system is composed basically of a PV generation system and a DVR (Fig. 1). For the cost evaluation, the main components are analyzed.

A. PV Generation System

The PV generation system is composed of a PV array, the dc link capacitors and a dc-ac converter. In the configurations used in this paper, the PV array is always composed of 7 panels in series in such a way that the ideal dc link voltage is around 120V. When a PV generation system is connected to the grid, it is important to have the dc link voltage higher than a single panel (17V) to allow a good control performance. The supply has a phase rms voltage of 220V, which means that a transformer (*L* in Fig. 2) is used. A turn ratio of 10:1 has been used to connect the system to grid.

Three possibilities of parallel connections have been tested to evaluate the cost for different generated PV power. There were considered PV arrays of 7 panels (700W), 14 panels (1400W) and 28 panels (2800W).

The dc link is composed of a capacitor of 300μF for all situations. Therefore the cost of this part of the system is kept constant. Also the cost of the dc capacitor is very low when compared to the PV array (Table I). All prices are in US$.

The PV converter is composed of six power switches with their gate drive circuits and heat sink. 200V MOSFETs have been used. The prices of transformers with turn ratio 10:1 were also considered in the total cost. The power ratings of the transformers were 600, 1500 and 3000VA for the PV array power of 700, 1400 and 2800W, respectively.

B. DVR System

The DVR system is composed of a dc-ac converter, a filter and a series transformer.

The DVR converter is composed of MOSFETs of 200V, 5A. The currents even during the voltage sag are much smaller than the currents of the PV converter.

The filter is composed of a 50μF capacitor and a 5mF inductor for all situations. The LC filter has a cut frequency of 318Hz that is approximately 5 times the grid frequency. Transformers with turn ratio 10:1 are also considered in the total cost. All prices shown in Table II are in US$.

The power ratings of the series transformers are 600VA for all conditions since the currents have small variation when the PV array power changes. It is worth noting that in the proposed system there are additional components, increasing the cost of the global system. Also the PV converter and the PV transformer must have higher ratings to support the higher values of currents during the voltage sag. However, due to the high cost of the PV array when compared with the other components used in the system, the additional cost can be justified.

The critical case for the cost of the additional system occurs for the PV array of 700W. In this case, the PV system has a total cost of approximately US$ 3,936 without voltage sag compensation.

TABLE I
PV system cost without voltage sag compensation

Components	Cost (US$) PV array power		
	700W	**1400W**	**2800W**
PV array	3,594	7,188	14,376
Dc capacitor	22	22	22
PV converter	82	132	322
PV transformer	238	287	369

TABLE II
PV system cost with voltage sag compensation

Components	Cost (US$) PV array power		
	700W	**1400W**	**2800W**
PV array	3,594	7,188	14,376
Dc capacitor	22	22	22
PV converter	132	210	396
PV transformer	271	336	450
DVR converter	82	82	82
DVR transform.	222	222	222
DVR filter	61	61	61

With voltage sag compensation, the cost is approximately US$ 4,384 that means an additional cost of 11.4%. Increasing the PV array power, the cost of the extra components becomes less significant for the system. For the PV array of 1,400W, the additional cost is 6.5% while for the PV array of 2,800W, the additional cost is only 1.1%.

The custom-power equipments are used in systems that can have a power up to 250KVA. As can be seen in Tables I and II, the cost of extra components becomes less significant when the power increases and therefore the power electronics components would not be a problem in systems of 250KVA. However, the cost of the PV arrays in this power range is extremely high and they can make the system unviable. A very large number of solar cells connected in series and parallel would have to be used to build the PV array.

VII. CONCLUSION

The proposed topology introduced in this paper improves functionality in grid connected photovoltaic generation systems. The system can be connected to a three-phase system of any electric utility if a matching transformer is used. The excellent performance of the system is verified from simulated results using Matlab. The voltage waveform in the photovoltaic array follows the reference voltage for all irradiation conditions. Besides that, the controller also compensates current harmonics and reactive power. A comparative study of PWM techniques is also presented.

The good performance of the DVR system is verified from simulated and experimental results. The voltage waveform in the load follows the reference voltage keeping the load voltage in the rated value. Cost estimation also has been performed. It is shown that the additional components are not significant for the total cost of the system, especially if the PV array power is high.

ACKNOWLEDGEMENT

The authors thank Conselho Nacional de Desenvolvimento Científico e Tecnológico (CNPq) for its financial support.

REFERENCES

[1] Y. C. Kuo, T. J. Liang, and J. F. Chen, "Novel maximum power-point-tracking controller for photovoltaic energy conversion system", *IEEE Trans. on Industrial Electronics*, vol. 48, no. 3, pp. 594-601, May/June 2001.

[2] L. G. Leslie, Jr., *Design and analysis of a grid connected photovoltaic generation system with active filtering function*, Master Thesis, Virginia Polytechnic Institute and State University, Blacksburg, Virginia – USA, 2003.

[3] H. Akagi, Y. Kanazawa and A. Nabae, "Instantaneous reactive power compensator comprising switching devices without energy storage components", *IEEE Trans. on Industry Applications*, vol. 20, no.3, pp. 625-630, May/June 1984.

[4] M. Aredes and E.H. Watanabe, "New control algorithms for series and shunt three-phase four-wire active power filters," *IEEE Trans. on Power Delivery*, vol. 10, no. 3, pp. 1649-1656, May/June 1995.

[5] A. Ghosh, A. K. Jindal, and A. Joshi, "A unified power quality conditioner for voltage regulation of critical load bus," *IEEE Power Engineering Society General Meeting*, pp. 471-476, 2004.

[6] M. Basu, S. P. Das, and G. K. Dubey, "Performance study of UPQC-Q for load compensation and voltage sag mitigation," *IEEE Annual Conference of the Industrial Electronics Society*, pp. 698-703, 2002.

[7] G. Jianjun, X. Dianguo, L. Hankui, and G. Maozhong, "Unified power quality conditioner (UPQC): the principle, control and application," *IEEE Power Conversion Conference*, pp. 80-85, 2002.

[8] H. Fujita and H. Akagi, "The unified power quality conditioner: the integration of series- and shunt-active filters," *IEEE Trans. on Power Electronics*, vol. 13, no. 2, pp. 315-322, March 1998.

[9] M. S. Yun, W. C. Lee, I. Suh, and D. S. Hyun, "A new control scheme of unified power quality compensator – Q with minimum power injection," *IEEE Annual Conference of the Industrial Electronics Society*, pp. 51-56, 2004.

[10] B. S. Chae, W. C. Lee, T. K. Lee, and D. S. Hyun, "A fault protection scheme for unified power quality conditioners," *IEEE International Conference on Power Electronics and Drive Systems*, pp. 66-71, 2001.

[11] H. Fujita and H. Akagi, "The unified power quality conditioner: the integration of series active filters and shunt active filters," *IEEE Power Electronics Specialists Conference*, pp. 494-501, 1996.

[12] M. Vilathgamuwa, Y. H. Zhang, and S. S. Choi, "Modeling, analysis and control of unified power quality conditioner," *IEEE International Conference on Harmonics and Quality of Power*, pp. 1035-1040, 1998.

[13] V. Khadkikar, P. Agarwal, A, Chandra, A. O. Barry, and T. D. Nguyen, "A simple new control technique for unified power quality conditioner (UPQC), *IEEE International Conference on Harmonics and Quality of Power*, pp. 289-293, 2004.

[14] L. F. C. Monteiro, M. Aredes, J. A. Moor Neto, "A control strategy for unified power quality conditioner,"

IEEE International Symposium on Industrial Electronics, pp. 391-396, 2003.
[15] M. Hu and H. Chen, "Modeling and controlling of unified power quality compensator," *International Conference on Advances in Power System Control*, pp. 431-435, 2000.
[16] B. Singh, K. Al-Haddad, and A. Chandra, "A review of active filters for power quality improvement," *IEEE Trans. on Industrial Electronics*, vol. 46, no. 5, pp. 960-971, September/October 1999.
[17] L. Gyugyi, C.D. Schauder, S.L. Williams, T.R. Rietman, D.R. Torgerson and A. Edris, "The unified power flow controller: a new approach to power transmission control," *IEEE Trans. on Power Delivery*, vol. 10, no. 2, pp. 1085-1093, March/April 1995.
[18] S. Moran, "A line voltage regulator/conditioner for harmonic sensitive load isolation," *IEEE Industry Applications Society Conference*, 1989, pp. 947-951.
[19] M. C. Cavalcanti, G. M. S. Azevedo, B. A. Amaral, K. C. de Oliveira, F. A. S. Neves, Z. D. Lins, "Efficiency evaluation in grid connected photovoltaic energy conversion systems," *IEEE Power Electronics Specialists Conference*, pp. 269-275, 2005.
[20] N. Mendalek and K. Al-Haddad, "Modeling and nonlinear control of shunt active power filter in the synchronous reference frame," *IEEE Harmonics and Quality of Power International Conference*, pp. 30-35, 2000.
[21] C. Hua, J. Lin, and C. Shen, "Implementation of a DSP-controlled photovoltaic system with peak power tracking," *IEEE Trans. on Industrial Electronics*, vol. 45, no. 1, pp. 99-107, January/February 1998.
[22] C.S. Chang, Y.S. Ho and P.C. Loh, "Voltage quality enhancement with power electronics based devices", *IEEE Power Engineering Society Winter Meeting*, vol. 4, pp. 2937-2942, 2000.
[23] O. Nóbrega Neto, L. F. C. Pimentel, M. C. Cavalcanti, F. A. S. Neves, C. L. Costa, and W. B. dos Santos, "A design guideline for dynamic voltage restorers," International Power Electronics and Motion Control Conference, 2004.
[24] A. M. Hava, R. J. Kerkman, and T. A. Lipo, "Simple analytical and graphical tools for carrier based pwm methods," *IEEE Power Electronics Specialists Conference*, pp.1462-1471, 1997.
[25] C. B. Jacobina, A. M. N. Lima, E. R. C. da Silva, R. N. C. Alves, and P. F. Seixas, "Digital scalar pulse width modulation: a simple approach to introduce non-sinusoidal modulating waveforms," *European Conference on Power Electronics and Applications*, pp. 100-105, 1997.
[26] M. C. Cavalcanti, E. R. C. da Silva, D. Boroyevich, W. Dong, and C. B. Jacobina, "Comparative evaluation of losses in soft and hard-switched inverters," *IEEE Industry Applications Society Conference*, pp. 1912-1917, 2003.

BIOGRAPHIES

Marcelo Cabral Cavalcanti was born in Recife, Brazil, in 1972. He received the B.S. degree in electrical engineering in 1997 from the Federal University of Pernambuco, Recife, Brazil, and the M.S. and Ph.D. degrees in electrical engineering from the Federal University of Campina Grande, Campina Grande, Brazil, in 1999 and 2003, respectively.

He was at the Center for Power Electronics Systems (CPES), Virginia Polytechnic Institute and State University, Blacksburg, USA from 2001 to 2002. Since 2003, he has been at the Electrical Engineering and Power Systems Department, Federal University of Pernambuco, where he is currently a Professor of Electrical Engineering. His research interests are: power electronics, renewable energy systems, and power quality.

Gustavo Medeiros de Souza Azevedo was born in Belo Jardim, Brazil, in 1981. He is currently working toward the B.S. degree in electrical engineering in the Federal University of Pernambuco, Recife, Brazil.

He has worked with the Power Electronics and Electrical Drives Group of the Federal University of Pernambuco. His research interests are power electronics and renewable energy systems.

Bruno de Aguiar Amaral was born in Recife, Brazil, in 1981. He received the B.S. degree in electrical engineering in 2005 from the Federal University of Pernambuco, Recife, Brazil, where he is currently working toward the M.S. degree in electrical engineering.

He has worked with the Power Electronics and Electrical Drives Group of the Federal University of Pernambuco. His research interests are power electronics and renewable energy systems.

Francisco de Assis dos Santos Neves was born in Campina Grande, Brazil, in 1963. He received the B.S. and M.S. degrees in electrical engineering in from the Federal University of Pernambuco, Recife, Brazil, in 1984 and 1992, respectively and the Ph.D. degree in electrical engineering in 1999 from the Federal University of Minas Gerais, Belo Horizonte, Brazil.

Since 1993, he has been at the Electrical Engineering and Power Systems Department, Federal University of Pernambuco, where he is currently a Professor of Electrical Engineering. His research interests are motor drives, power electronics, renewable energy systems and power quality.

Davi Carvalho Moreira was born in Tucuruí, Brazil, in 1982. He received the B.S. degree in electrical engineering from the Federal University of Pernambuco, Recife, Brazil, in 2004, where he is currently working toward the M.S. degree in electrical engineering.

He has worked with the Power Electronics and Electrical Drives Group of the Federal University of Pernambuco. His research interests are motor drives and power electronics.

Kleber Carneiro de Oliveira was born in Recife, Brazil, in 1980. He received the B.S. degree in electrical engineering in 2005 from the Federal University of Pernambuco, Recife, Brazil, where he is currently working toward the M.S. degree in electrical engineering.

He has worked with the Power Electronics and Electrical Drives Group of the Federal University of Pernambuco. His research interest is power electronics and renewable energy.